

Seismo-electric Conversion in Sandstones and Shales using Two Different Experimental Approaches, Modelling and Theory

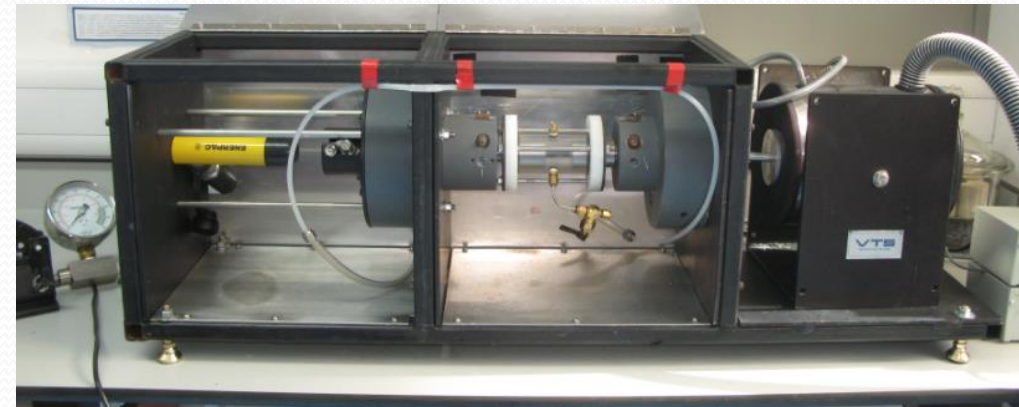
Paul W.J. Glover, Piroska Lorinczi, Rong Peng, Bangrang Di

Frequency-dependent processes

- ❖ Electro-kinetic processes link hydraulic flow, electrical flow and the passage of elastic waves through porous media.
- ❖ Passage of elastic waves causes fluid to flow, and that flow gives rise to an electrical streaming potential and electrical counter-current.
- ❖ These processes are frequency-dependent and governed by coupling coefficients which are themselves frequency-dependent.
- ❖ The link between fluid pressure and fluid flow is described by dynamic permeability, which is characterised by the hydraulic coupling coefficient (C_{hp}).
- ❖ The link between fluid pressure and electrical streaming potential is characterised by the streaming potential coefficient (C_{sp}).

- ❖ While the steady-state values of such coefficients are well studied and understood, their frequency dependence is not.
- ❖ Previous work has been confined to unconsolidated and disaggregated materials such as sands, gravels and soils.
- ❖ In this work we present two apparatuses for measuring the hydraulic, streaming potential and electroseismic coefficients of high porosity, high permeability consolidated porous media and shales as a function of frequency.

- ❖ The apparatus operates in the range 1 Hz to 2 kHz with a sample of 10 mm diameter and 5 to 30 mm in length.
- ❖ The full design and validation of the apparatus is described together with the experimental protocol it uses.
- ❖ Initial data is presented for three samples of Boise sandstone, which present as disersive media with the critical transition frequency of 918.3 ± 99.4 Hz.
- ❖ The in-phase and in-quadrature components of the measured hydraulic and streaming potential coefficients have been compared to the Debye type dispersion model as well as theoretical models based on bundles of capillary tubes and porous media.



The Seismoelectric Apparatus

- ❖ The apparatus operates in the range 1 Hz to 2 kHz with a sample of 10 mm diameter and 5 to 30 mm in length.
- ❖ The full design and validation of the apparatus is described together with the experimental protocol it uses.
- ❖ Initial data is presented for three samples of Boise sandstone, which present as dispersive media with the critical transition frequency of 918.3 ± 99.4 Hz.
- ❖ The in-phase and in-quadrature components of the measured hydraulic and streaming potential coefficients have been compared to the Debye type dispersion model as well as theoretical models based on bundles of capillary tubes and porous media.

Theoretical Models

Theoretical models for coupling coefficients valid for:

- capillary bundles (Packard, 1953; Reppert et al., 2001)
- porous media (Pride, 1994; Walker and Glover, 2015)
- both as a function of frequency
- and including in-phase and in-quadrature components

For Bundles of Capillary Tubes (Packard Models)

The hydraulic coupling coefficient (C_{hp}) is expressed in velocity of flow per pressure difference, which is related to the dynamic permeability, and is given by (Packard, 1953)

$$C_{hp} = \frac{v(\omega)}{\Delta P(\omega)} = \frac{1}{\eta l \kappa^2} \left[\frac{2 J_1(\kappa a)}{\kappa a J_0(\kappa a)} - 1 \right], \quad \text{where } \kappa = \sqrt{\frac{-i\omega\rho}{\eta}},$$

and where l and a are the length and the radius of the capillaries (in m), and J_1 and J_0 are Bessel functions of the first and zeroth kind, respectively.

The streaming potential coefficient can also be obtained from Eq. (1) as (Packard, 1953)

$$C_{sp} = \frac{\Delta V(\omega)}{\Delta P(\omega)} = \frac{\varepsilon \zeta}{\eta \sigma} \left[\frac{-2 J_1(\kappa a)}{\kappa a J_0(\kappa a)} \right], \quad \text{where } \kappa = \sqrt{\frac{-i\omega\rho}{\eta}},$$

and where ε is the fluid permittivity (in F/m), ζ is the zeta potential (in V), and σ is the electrical conductivity of the fluid (in S/m)

For Porous Media

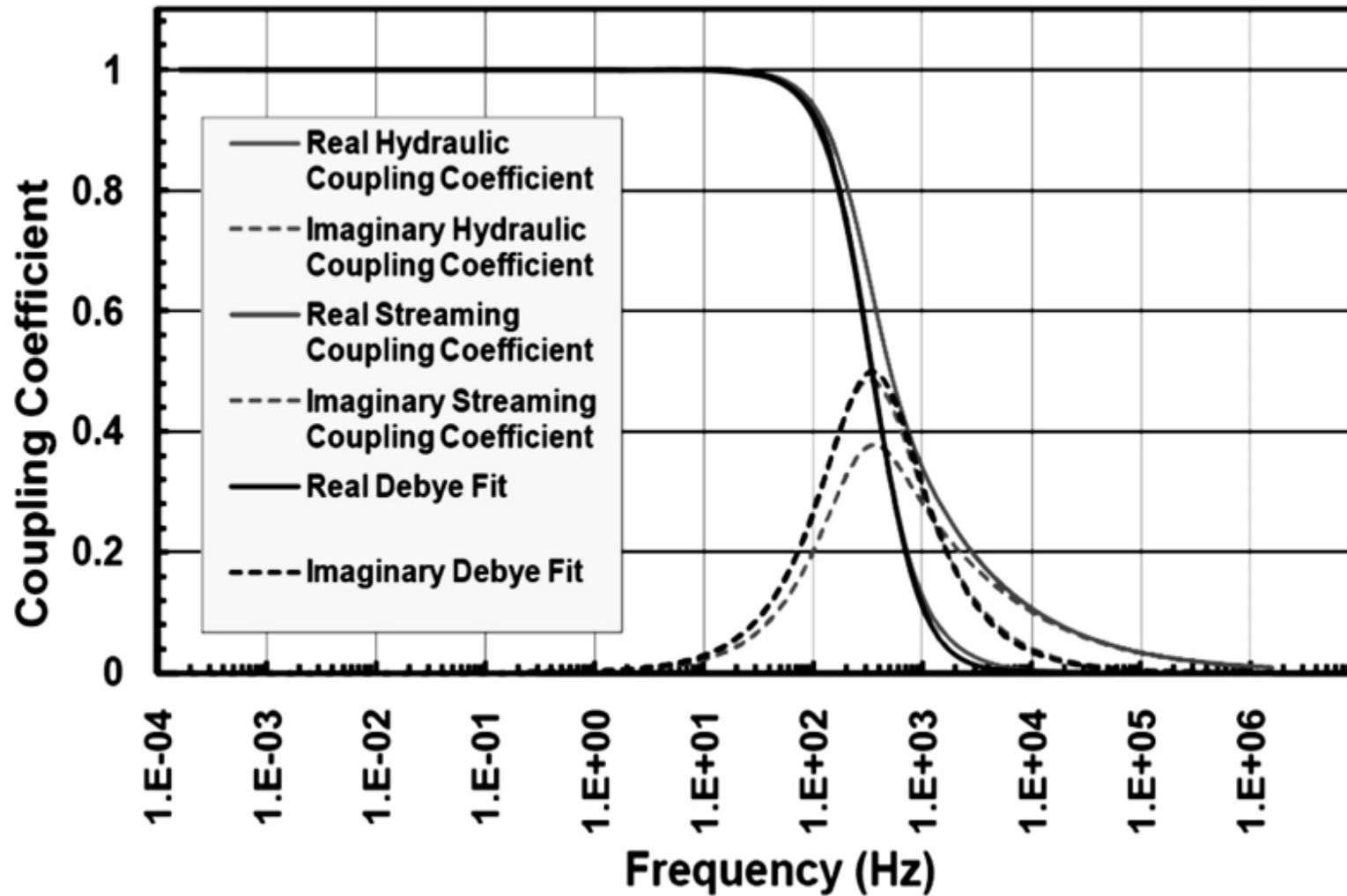
While the previous equations were derived for bundles of capillary tubes, [Pride \(1994\)](#) provided an equation for streaming potential coupling coefficient for porous media that is based on the theory of the electric double layer

$$C_{sp} = \frac{\Delta V(\omega)}{\Delta P(\omega)} = \frac{\varepsilon \zeta}{\eta \sigma} \left[1 - i \frac{\omega}{\omega_t} \frac{m^*}{4} \left(1 - \frac{2}{\delta \Lambda} \right)^2 \left(1 - i^{3/2} \sqrt{\frac{\omega \rho}{\eta}} \right)^2 \right]^{-1/2}, \quad \text{where } m^* = \frac{\phi \Lambda^2}{\tau_e k_{DC}},$$

where ω_t is the critical (transition) frequency (in rads/s), δ is the Debye length (in m) (see [Glover, 2015](#)), Λ is the characteristic pore size (in m), k_{DC} is the steady state permeability (in m²) and τ_e is the electrical tortuosity ($\tau_e = \phi^{1-m}$, where m is the cementation exponent (see [Glover, 2015](#))).

[Walker and Glover \(2010\)](#) provided a simplification of [Eq. \(4\)](#) for the case where $\Lambda \gg \delta$, i.e., when the pore fluid is medium to high salinity. Since the experiments carried out in this work were for pore fluids of a salinity $C_f = 0.1$ mol/dm³, the Pride model and its simplification provide almost identical values.

Frequency dependence of models



In-phase and in-quadrature components both vary with frequency

Relaxation models such as the Debye model may also be fitted to data

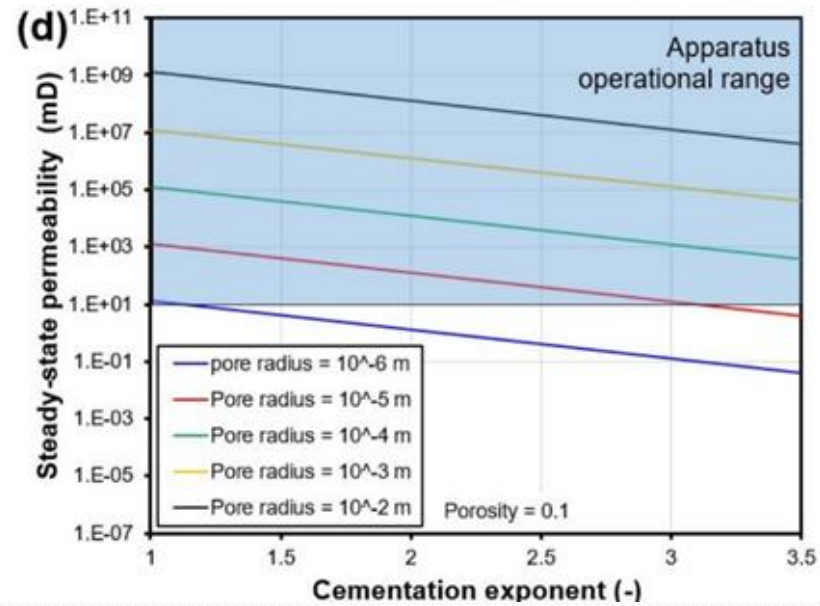
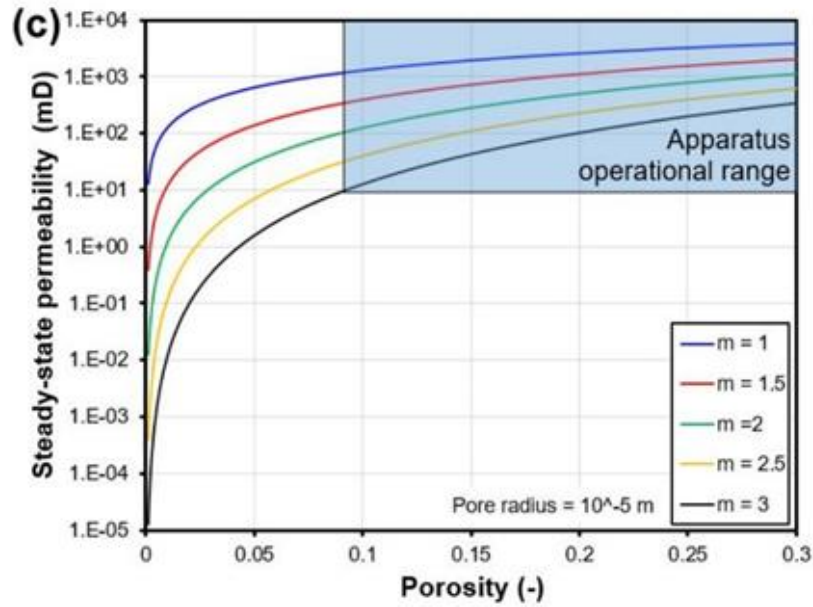
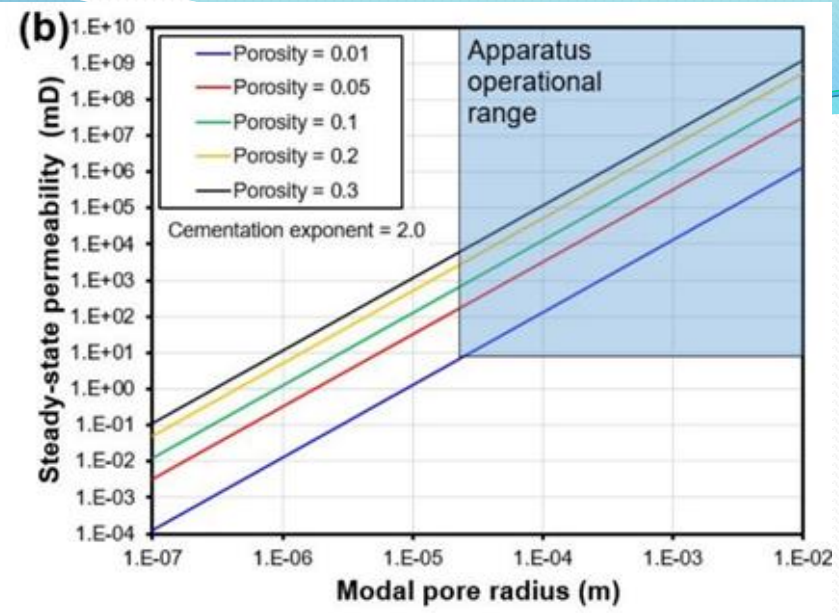
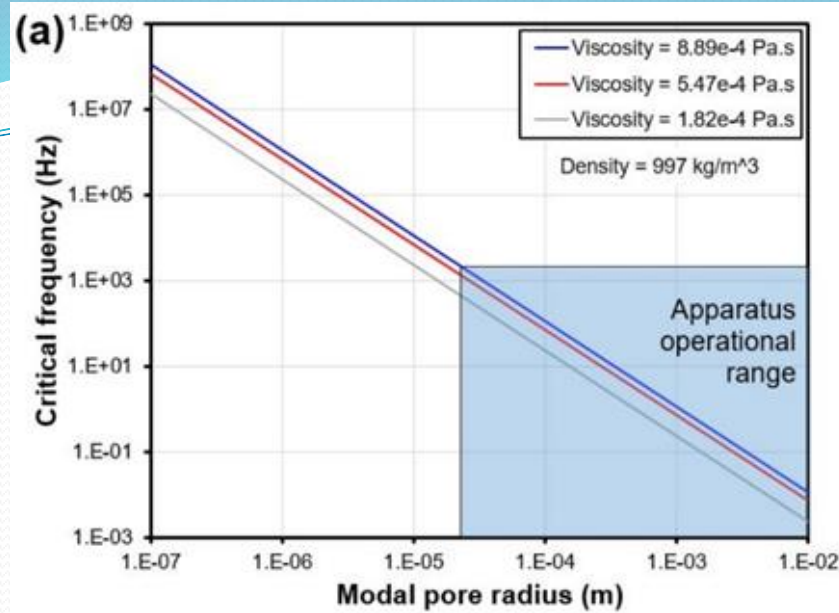
Dynamic Permeability and Streaming Potential Apparatus

An apparatus to measure:

- the AC streaming potential coupling coefficient
- dynamic permeability
- both as a function of frequency

Fine control of frequency allows measurements to be specific to the particular frequency

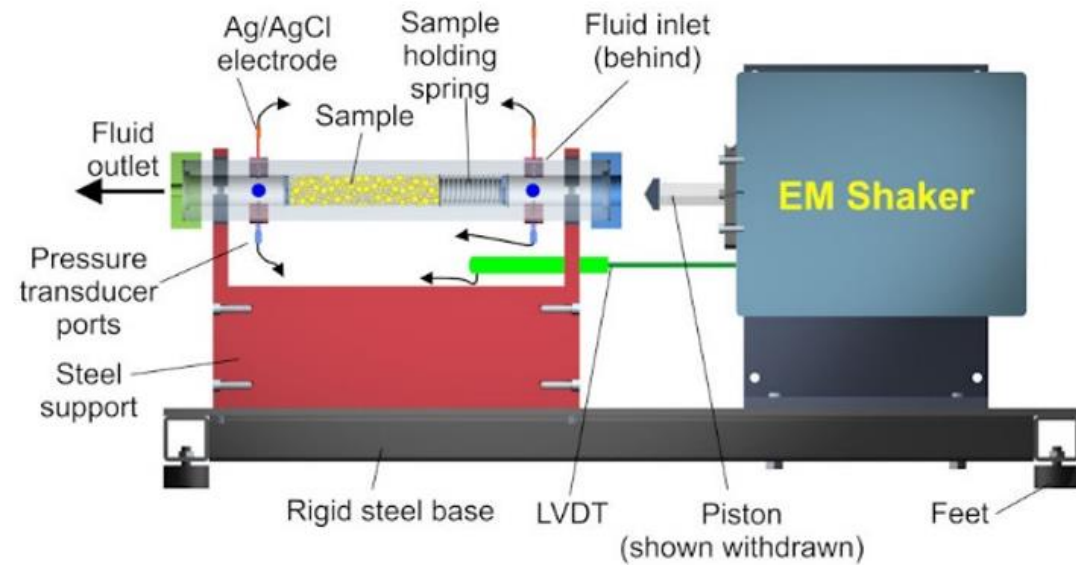
Apparatus Operational Ranges



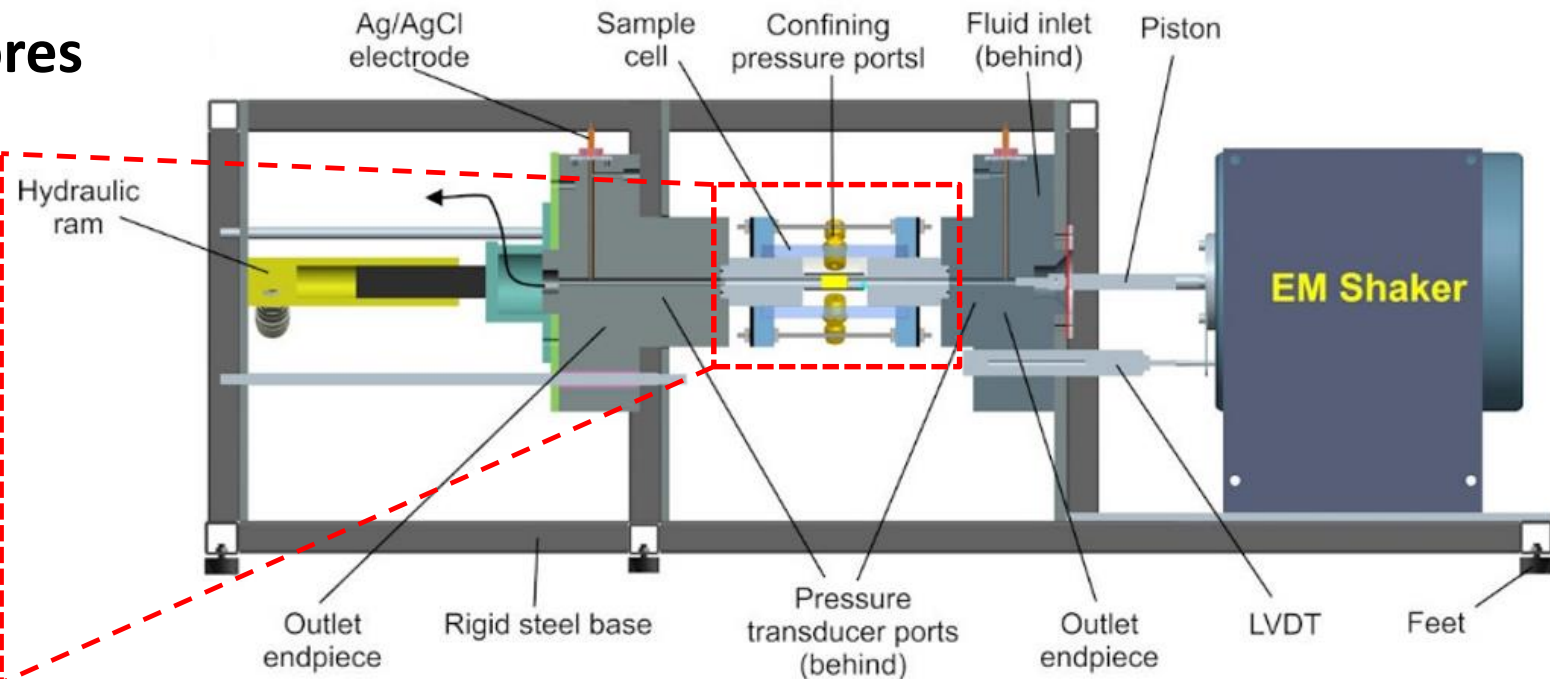
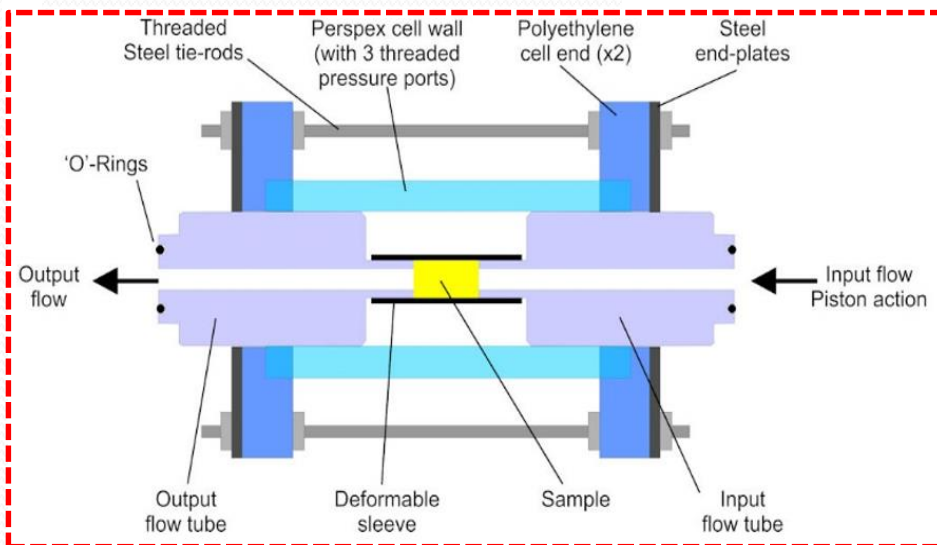
Measurements may be accurately made for a restricted range of pore radius, critical frequency, permeability, porosity and cementation exponent

The Apparatus

Existing Apparatus for Sands & Soils

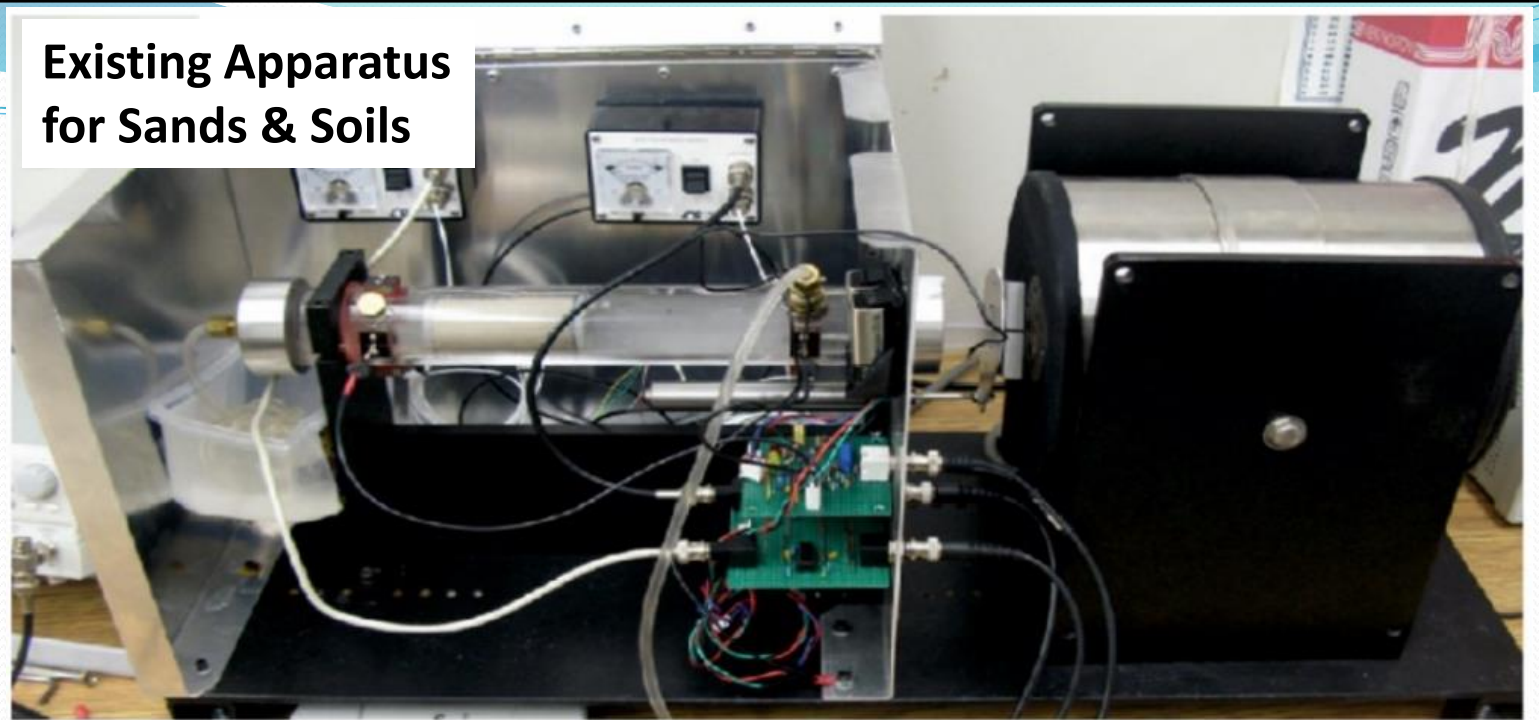


New Apparatus for solid cores

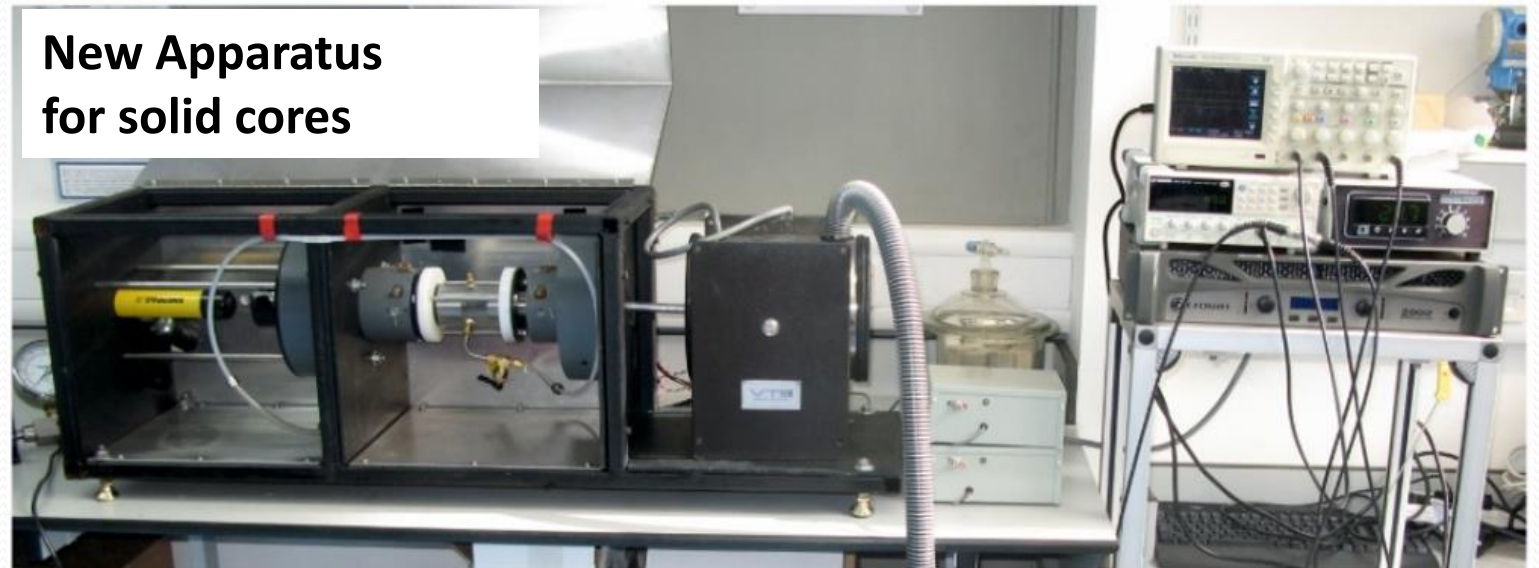


Laboratory Set-up

Existing Apparatus for Sands & Soils



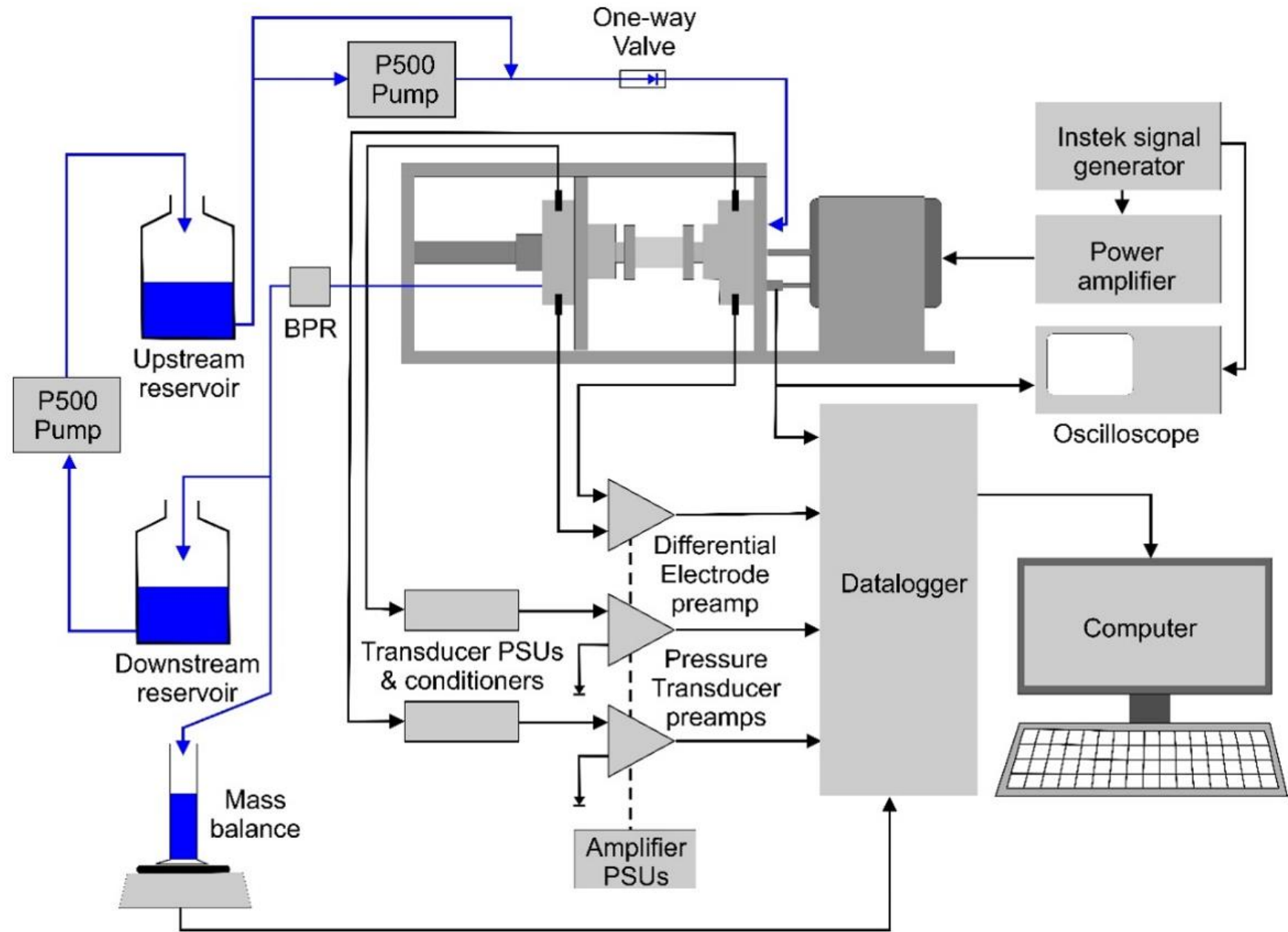
New Apparatus for solid cores



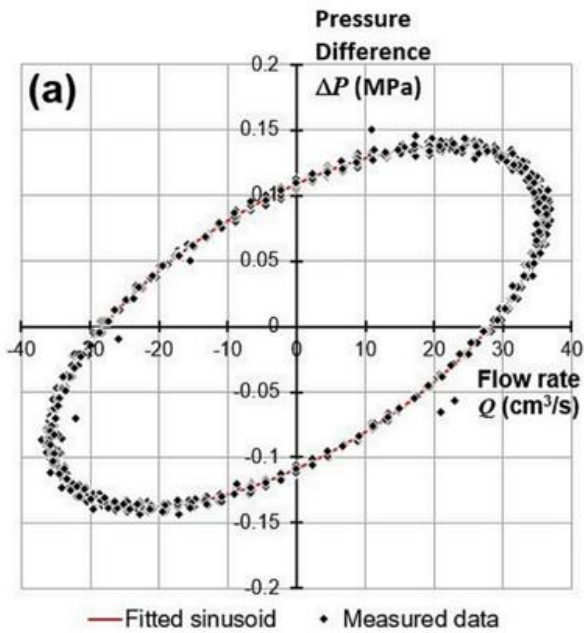
Instrumentation

Pressure transducers and specially-built preamps designed to accommodate high frequencies

Power amplifier to drive shaker is of HiFi quality

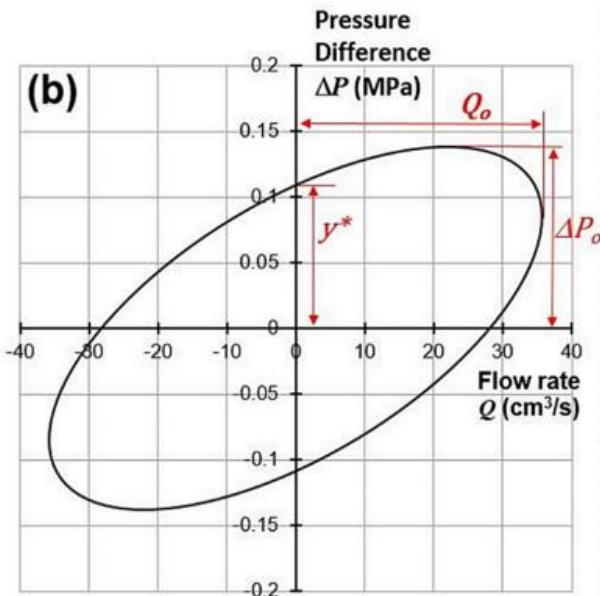
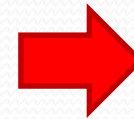


Data Analysis

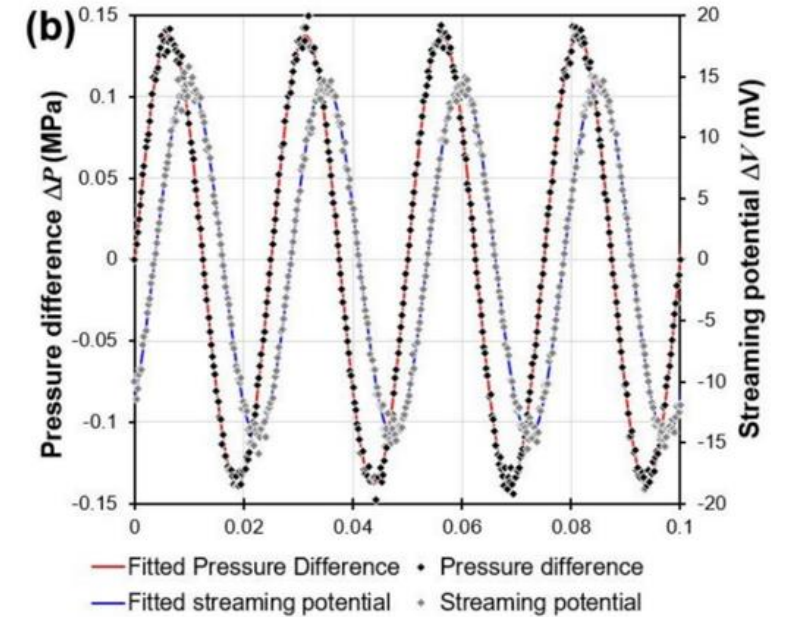
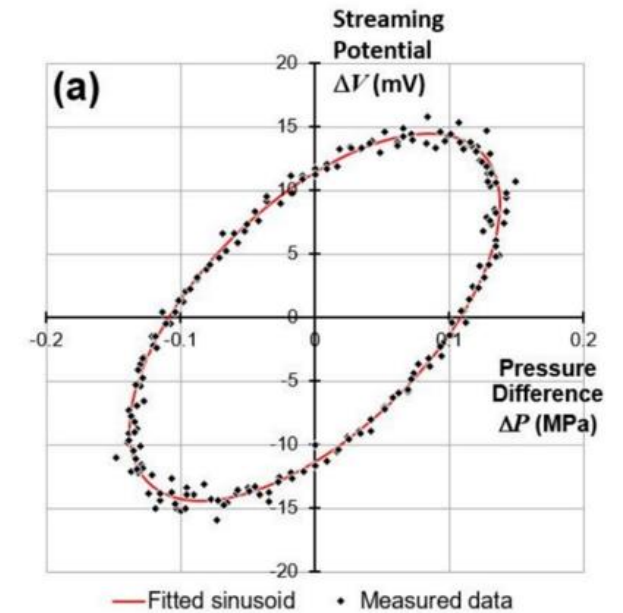


Carried out by
Lissajous theory

or sinusoidal fitting



Sinusoidal fitting provides marginally better results for both dynamic permeability and streaming potentials due to the large number of cycles which may be analysed.



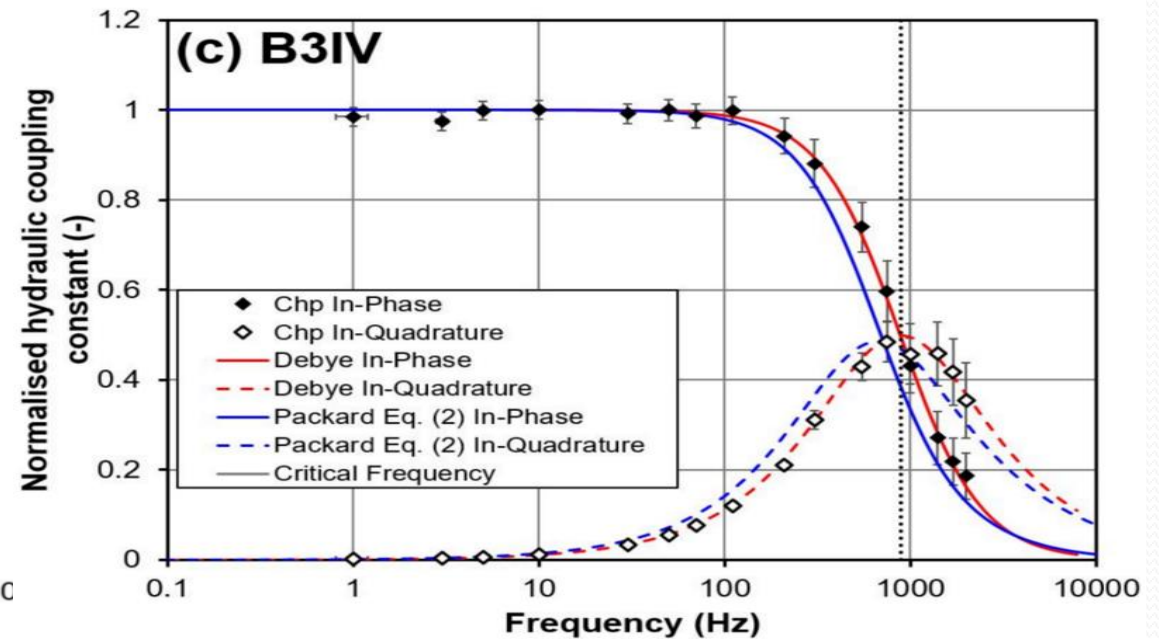
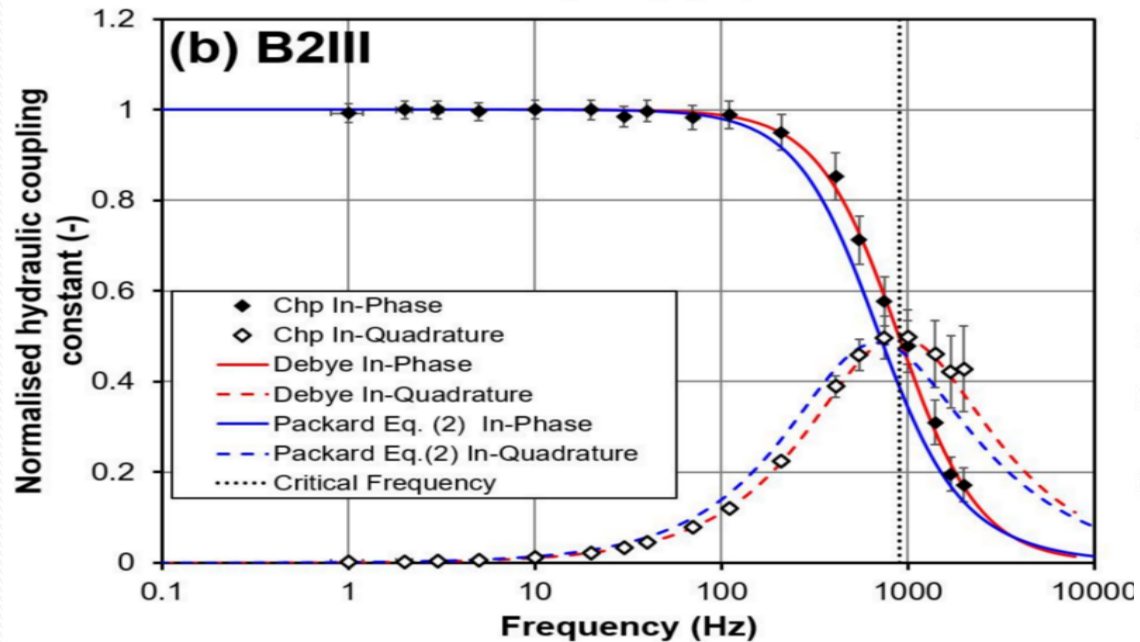
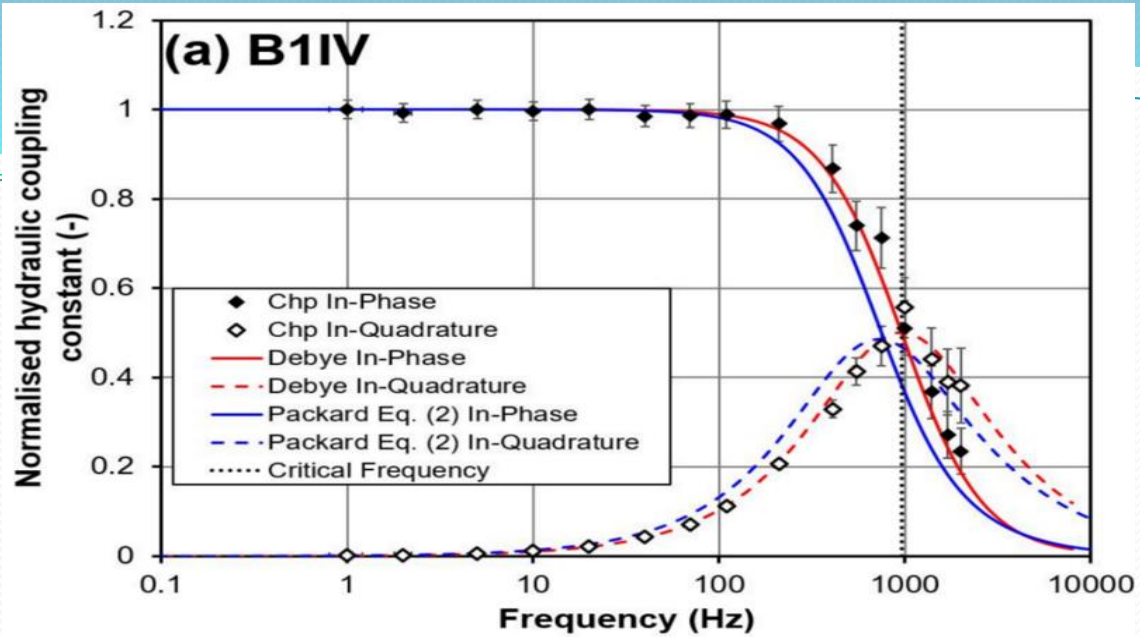
Dynamic Permeability and Streaming Potential Results

Frequency dependent results for 3 samples of Boise sandstone, including:

- Hydraulic coupling coefficient
- Streaming potential coupling coefficient
- Model fitting
- Critical frequency
- Characteristic pore radius measurement
- for permeability prediction

Hydraulic Coupling Coefficients with relevant fitted theoretical curves

- Symmetric dispersion
- Fitted better by the Debye relaxation than the Packard model
- Critical Frequency = 858-958 Hz
- Characteristic pore radius = 29 – 36 μm



SP Coupling Coefficients

with relevant fitted theoretical curves

- Assymmetric dispersion
- Not fitted by Debye relaxation or Packard models
- Fitted best by the Pride/Walker and Glover model
- Critical Frequency = 895-965 Hz
- Characteristic pore radius = 34.3 – 35.6 μm

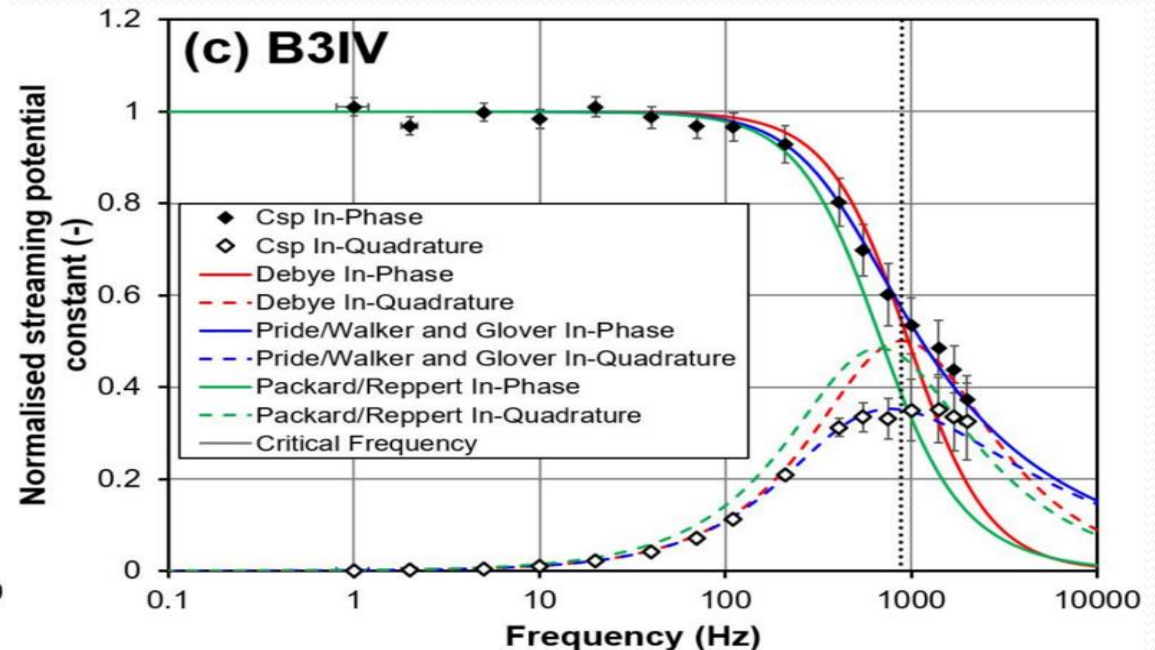
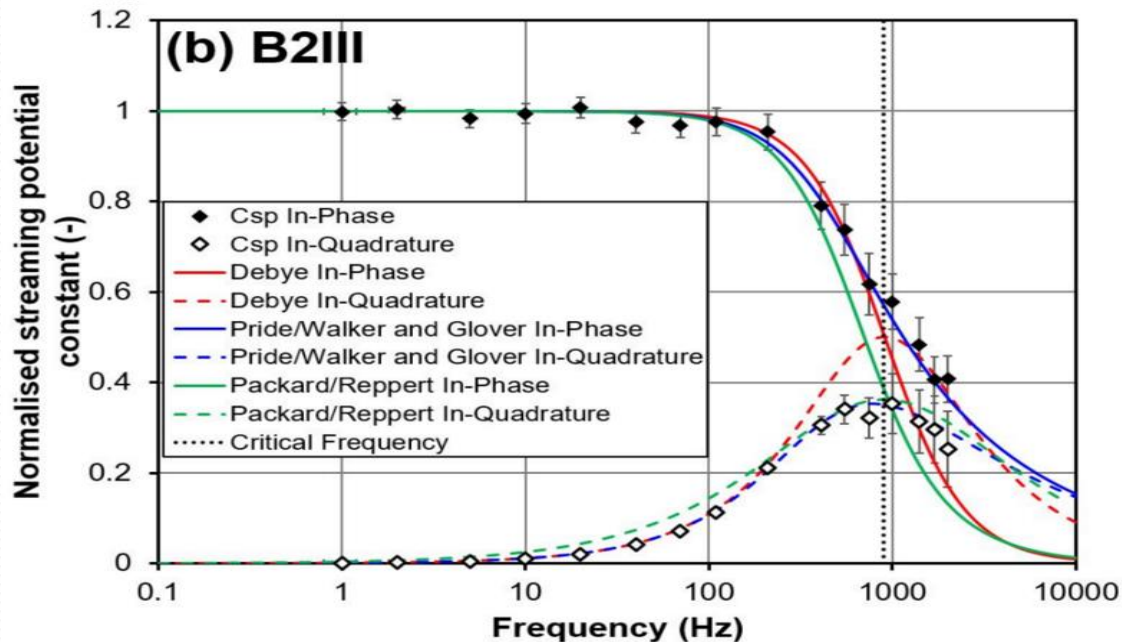
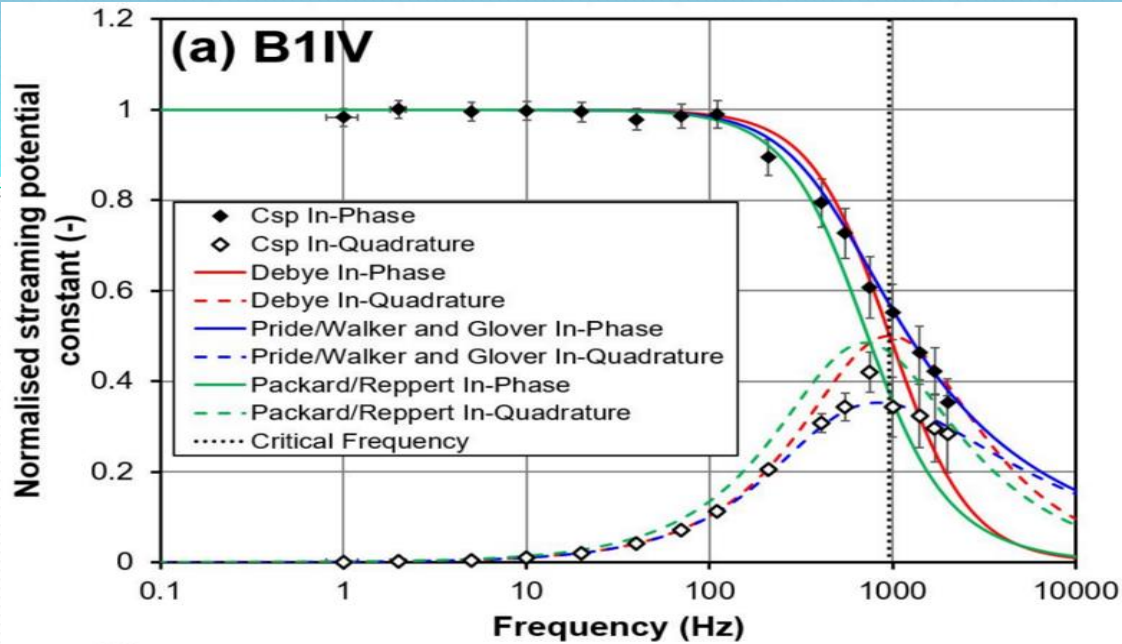


Table 3. Basic petrophysical characteristics of the sample material.

Variable	Units	B1IV	B2III	B3IV
Modal grain size (laser diffractometry)	$\times 10^{-6}$ m	221	223	209
Modal pore throat size (MICP)	$\times 10^{-6}$ m	21.1	22.2	21.5
Modal pore size r_{eff} [calculated, Glover and Walker (2009)]	$\times 10^{-6}$ m	33.9	34.97	35.3
Modal pore throat size [calculated, Glover and Déry (2010)]	$\times 10^{-6}$ m	20.5	21.1	21.3
Cementation exponent	(-)	1.629	1.677	1.651
Formation factor using m and ϕ_{sat}	(-)	6.92	6.59	6.21
Helium porosity	(-)	0.299	0.296	0.305
Saturation porosity	(-)	0.305	0.325	0.331
Mercury porosity	(-)	0.284	0.279	0.242
Surface conductivity	$\times 10^{-4}$ S/m	13.6	32	13.4
Fluid pH during measurement	(-)	7.2	6.94	6.61
Measured permeability (High salinity)	$\times 10^{-12}$ m ²	5.275	5.872	6.033
Fluid density	kg/m ³	997	997	997
Fluid viscosity	Pa.s	8.90E-04	8.90E-04	8.90E-04
Predicted f_{crit} from effective pore radius	Hz	986	929	910
f_{crit} from Debye fit to measured C_{hp} data (Figure 8)	Hz	958±45	898±45	885±45
r_{eff} from Debye fit to measured C_{hp} data (Figure 8)	$\times 10^{-6}$ m	34.4±1.5	35.6±1.5	35.8±1.5
r_{eff} from Packard fit to measured C_{hp} data (Figure 8)	$\times 10^{-6}$ m	29.0±1.7	31.0±1.7	31.0±1.7
f_{crit} from Pride/Walker and Glover fit to measured C_{sp} data (Figure 9)	Hz	965±65	909±65	895±65
r_{eff} calculated using Eq. (5) from Pride/Walker and Glover f_{crit} value	$\times 10^{-6}$ m	34.3±2.4	35.4±2.4	35.6±2.4

- An apparatus for the measurement of the streaming potential coefficient of high permeability porous media including high porosity rocks has been designed, constructed and tested.
- The apparatus can also be used to measure the dynamic permeability of high permeability porous media.
- The apparatus may be used for frequencies between 1 Hz and 2 kHz, for cylindrical samples of 10 mm and lengths between 5 mm and 30 mm. The lower limit of permeability is 10 mD ($9.869 \times 10^{-15} \text{ m}^2$), for which short samples must be used.
- Dynamic permeability can be measured to within $\pm 6.1\%$, and streaming potential coefficient to within $\pm 9.2\%$.
- The apparatus has been used to obtain data on three samples of Boise sandstone.

Summary of the Harmonic Approach 2

- The critical frequency was explicitly measurable on the high permeability Boise sandstone, which was 918.3 ± 99.4 Hz ($\pm 9.24\%$) overall, but less than $\pm 3.4\%$ for individual samples.
- Characteristic pore radius were both calculated from the critical frequencies and compared well with independent experimental measurements.
- Fits of the Debye model to C_{hp} data and the Pride model to C_{sp} data enabled the calculation of characteristic pore size to within 2%, while fits of the Packard model to C_{hp} data were 12% underestimated.
- While the restriction for using this apparatus only on high permeability porous media strictly limits the apparatus in geosciences, these measurements may find a greater application in chemical engineering where high porosity and permeability porous media are more common.

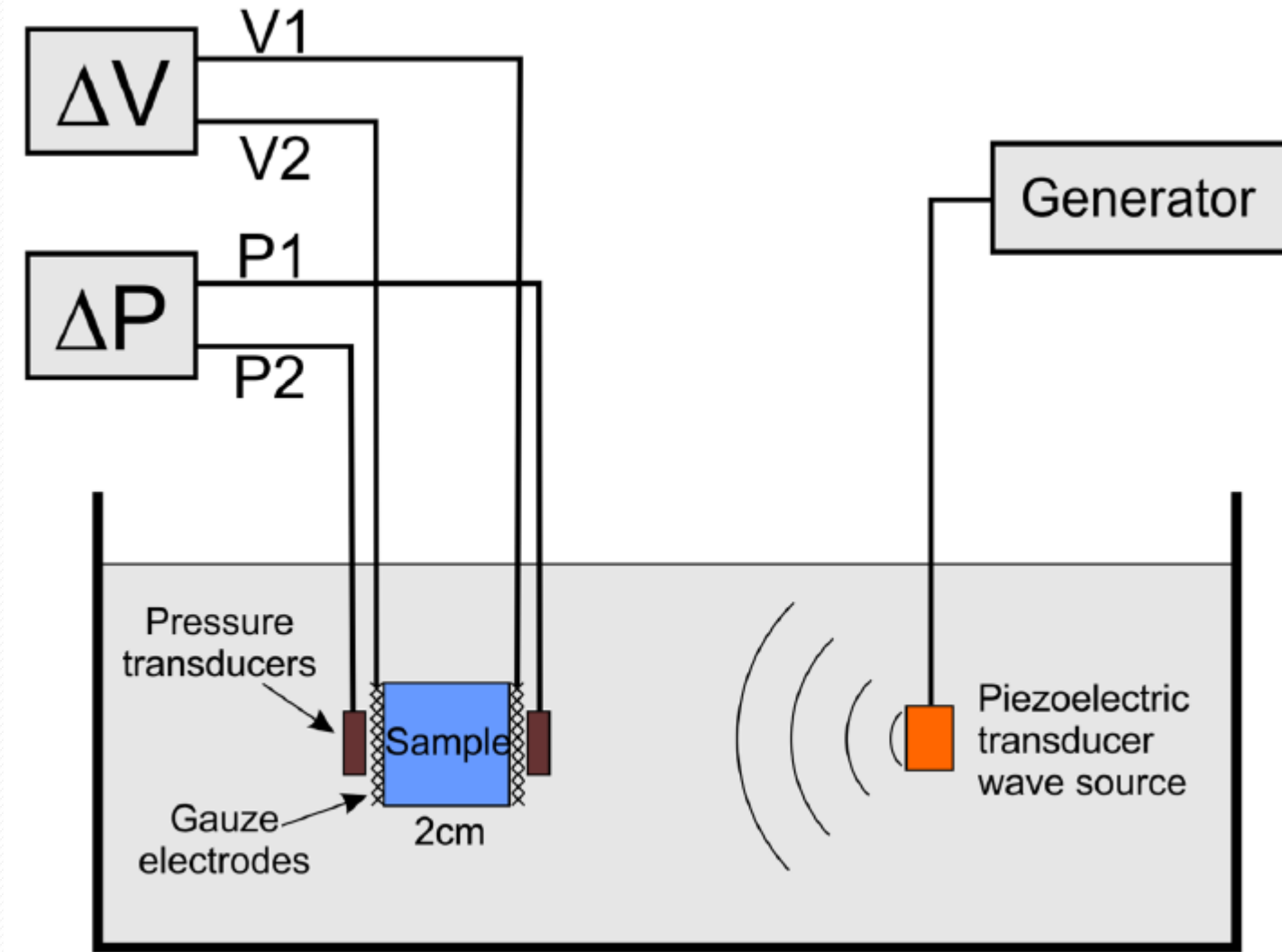
Seismoelectric Apparatus

An apparatus to measure:

- the seismoelectric coupling coefficient
- as a function of frequency
- using 28 natural samples, and
- 4 synthetic samples in 10 configurations

Use of natural and synthetic samples allows effects of porosity, permeability and frequency to be assessed.

Diagram of the apparatus

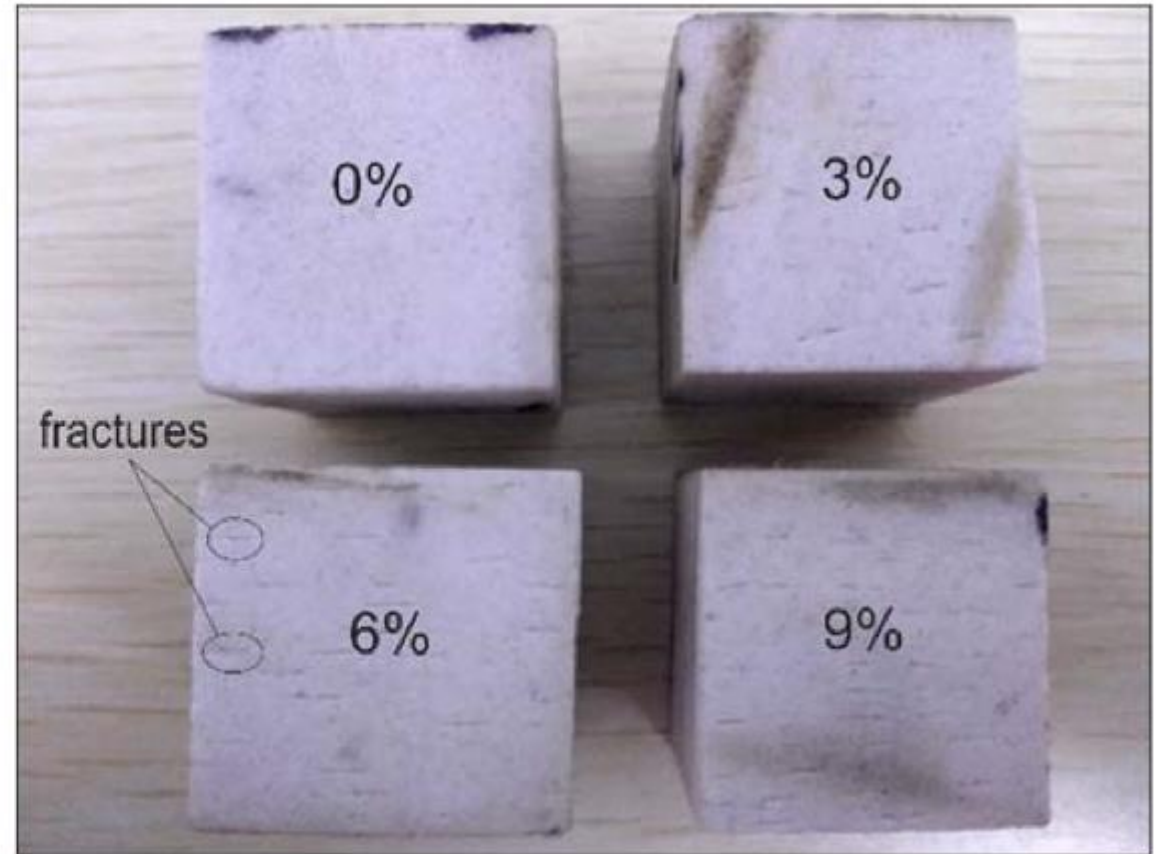


The passage of an elastic wave across the sample generates a fluid pressure difference ΔP , which causes fluid flow and a potential difference ΔV .

Natural Samples

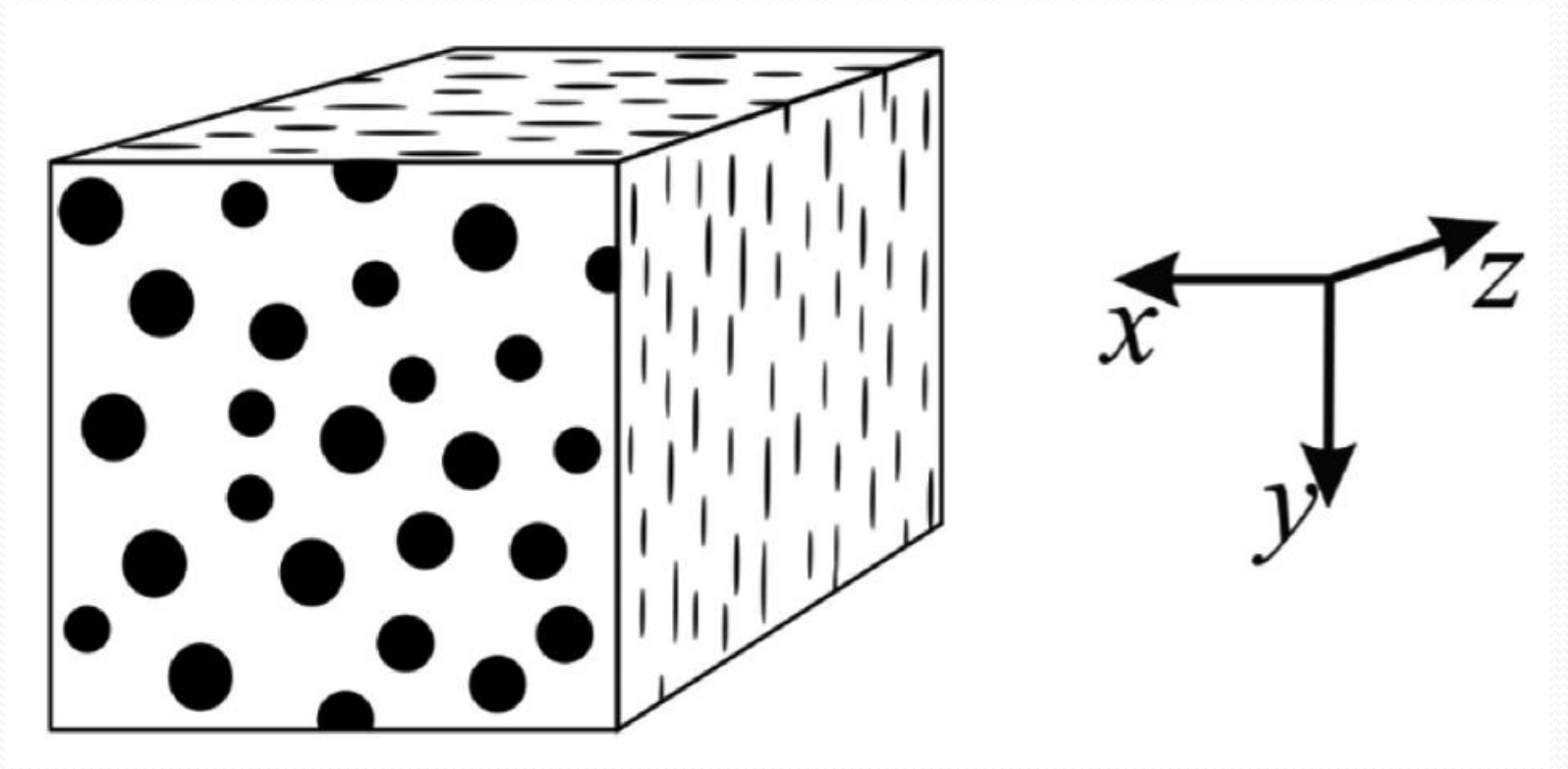


Synthetic Samples



Synthetic Samples

Synthetic samples can be created to be fracture free (A1), or have fractures to different degrees in different directions



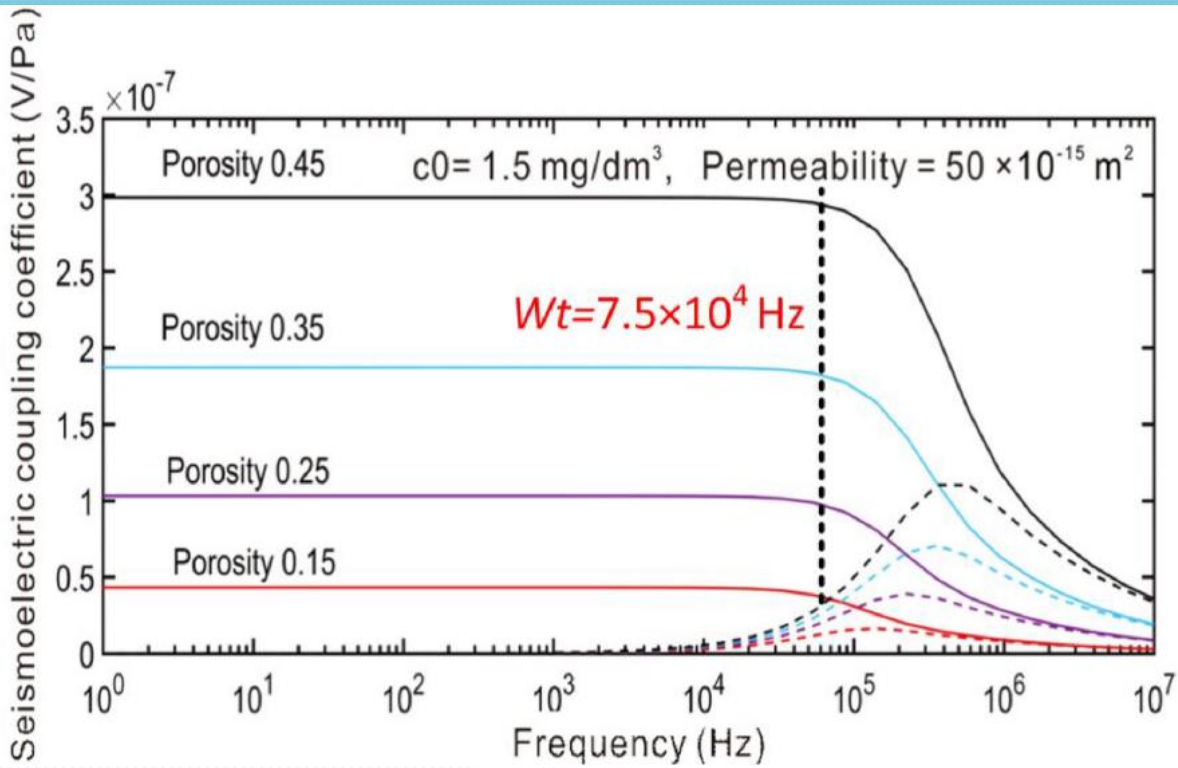
Sample number	Porosity (per cent)	Permeability ($\times 10^{-15} \text{m}^2$)	Sample number	Porosity (per cent)	Permeability ($\times 10^{-15} \text{m}^2$)
N1	10.84	0.001	N15	11.75	0.263
N2	13.44	0.002	N16	10.88	0.506
N3	12.40	0.004	N17	10.37	0.624
N4	12.15	0.007	N18	12.24	1.192
N5	15.98	0.020	N19	14.11	2.161
N6	10.96	0.023	N20	10.00	3.590
N7	12.16	0.025	N21	12.60	11.450
N8	10.93	0.034	N22	16.30	13.135
N9	13.03	0.079	N23	9.92	13.291
N10	9.91	0.090	N24	12.54	19.090
N11	12.92	0.117	N25	14.20	32.828
N12	13.62	0.122	N26	14.23	48.100
N13	11.29	0.134	N27	16.17	57.400
N14	15.05	0.259	N28	11.94	69.488
A1	23.8	310.79	A3y	23.8	1696.30
A2x	23.8	847.21	A3z	23.8	370.43
A2y	23.8	876.10	A4x	23.8	2053.27
A2z	23.8	325.53	A4y	23.8	2164.32
A3x	23.8	1509.34	A4z	23.8	427.39

Notes: Samples labelled N are natural rock samples, and those labelled A are artificial fractured sandstones. A1 is the sandstone without cracks, while the labels x, y and z represent the direction of wave propagation as defined in Fig. 3. The porosity is effective porosity acquired by helium porosimetry measurements. Permeability is Klinkenberg-corrected permeability (Klinkenberg 1941).

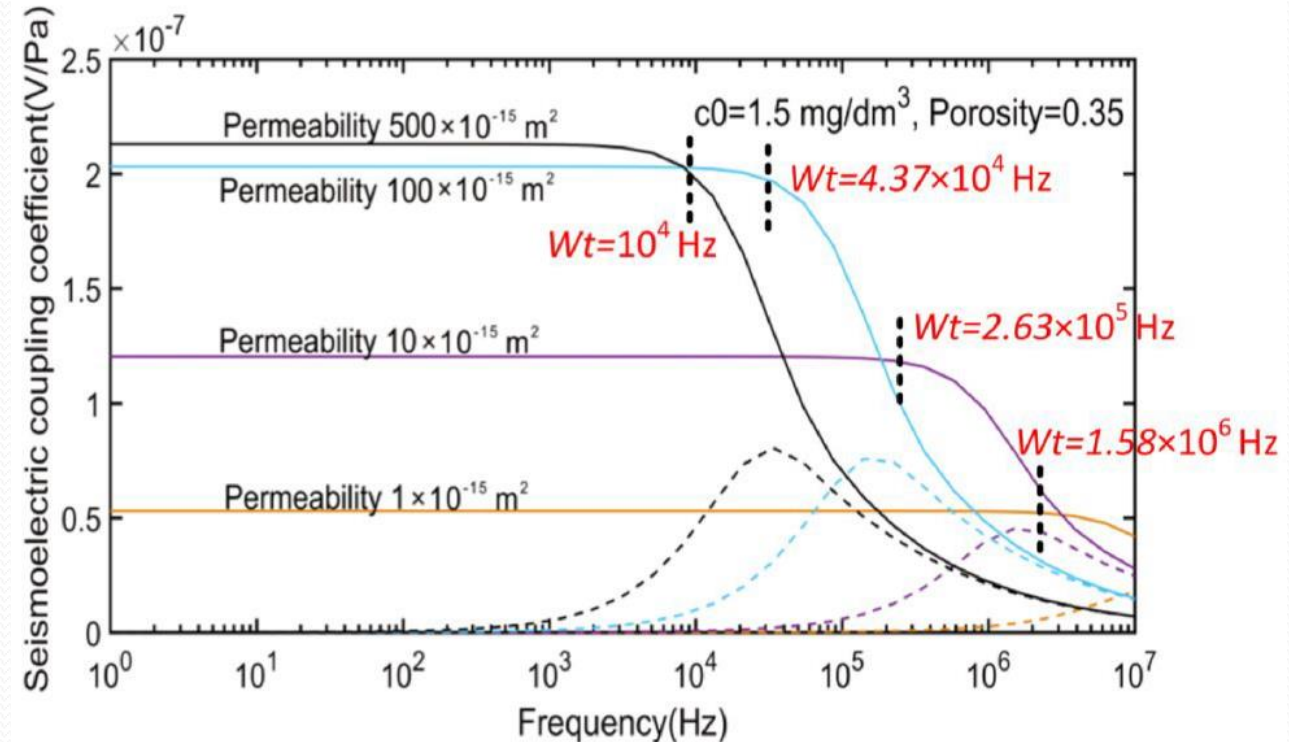
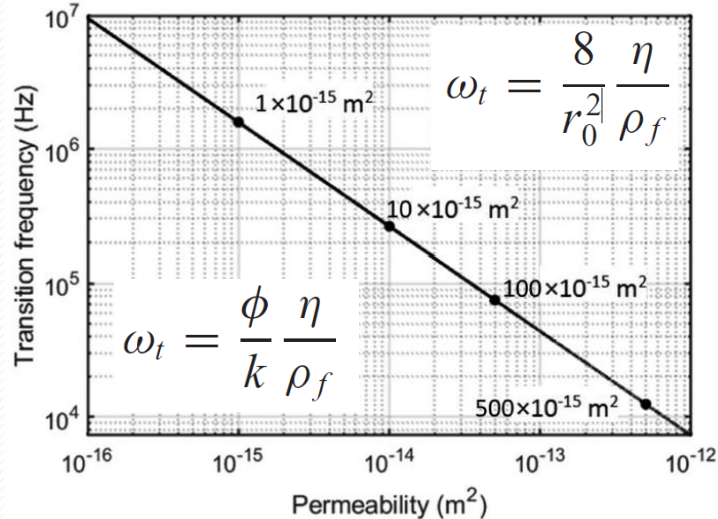
Theoretical Modelling

(using the Packard, 1953 capillary bundle model)

- Expected dependence of seismoelectric coupling coefficient with porosity and permeability

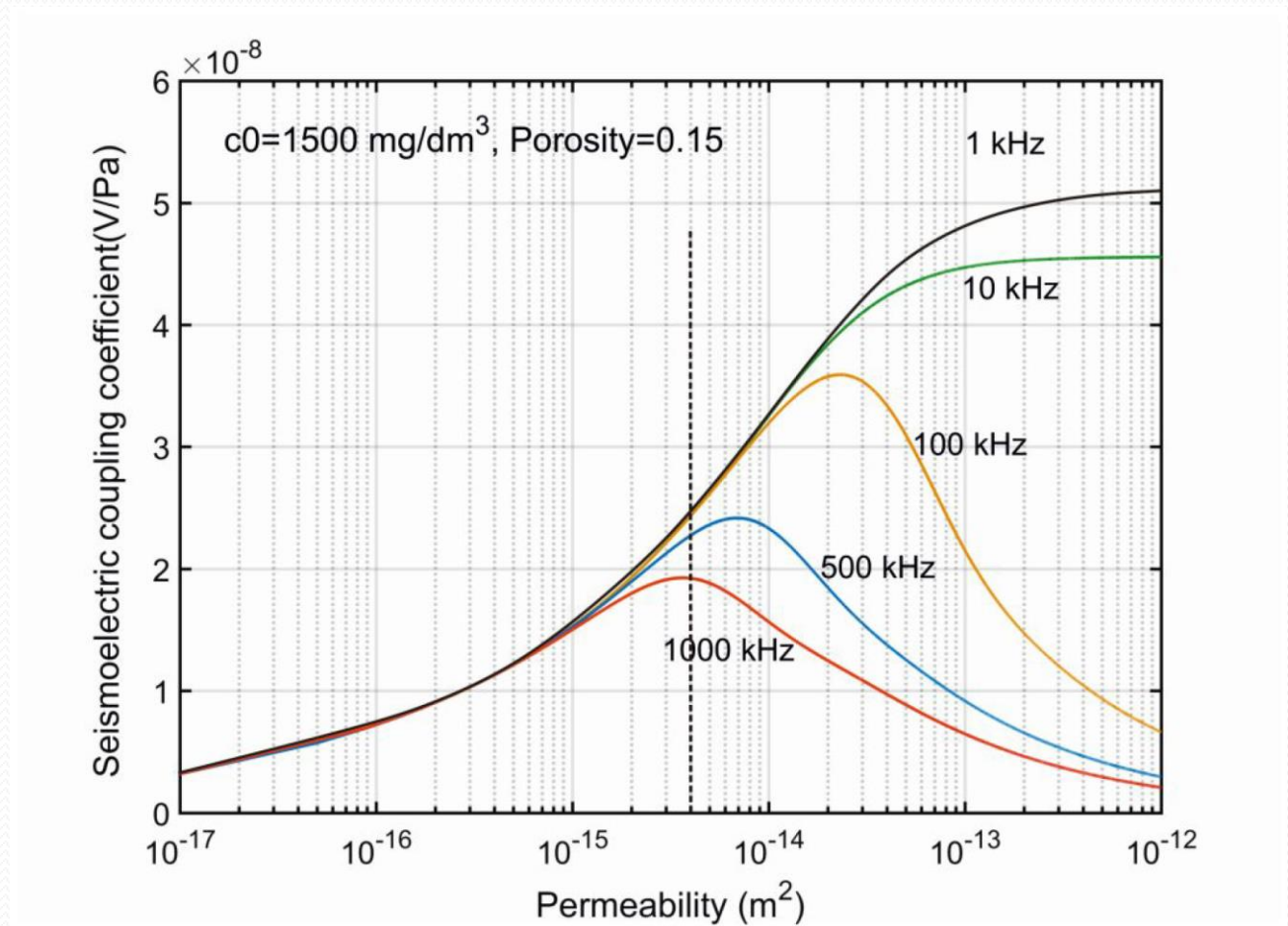


- Expected dependence of critical frequency on porosity and permeability



Modelled Seismoelectric Coupling Constant as a Function of Permeability and Frequency

- Seismoelectric Coupling Constant is closely dependent on both frequency and on permeability for rocks with permeabilities greater than about $2 \times 10^{-15} \text{ m}^2$



Seismoelectric Results

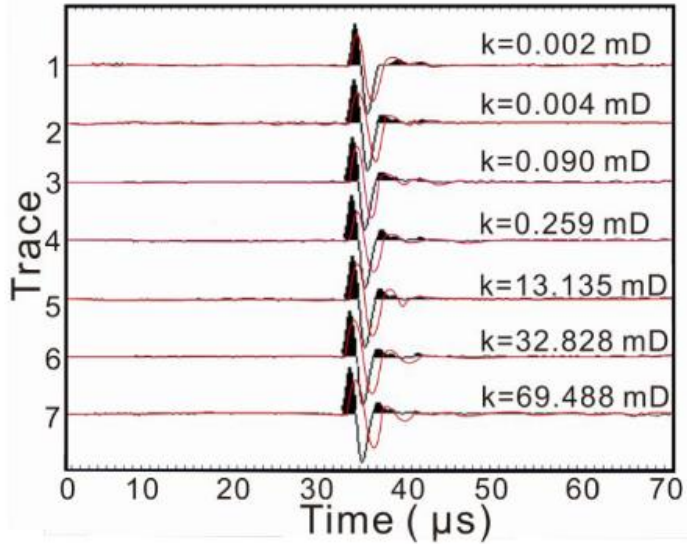
Experimental results for:

- the seismoelectric coupling coefficient
- as a function of frequency
- porosity, and
- permeability

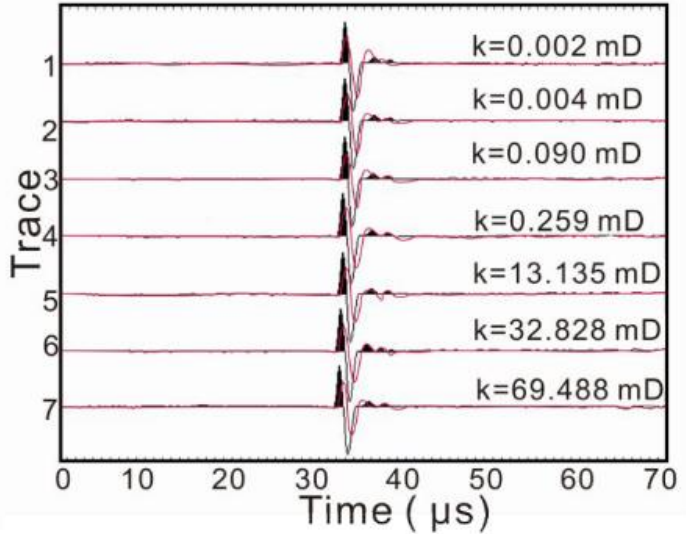
Use of natural and synthetic samples allows effects of porosity, permeability and frequency to be assessed.

Recorded Pressure and Potential Signals

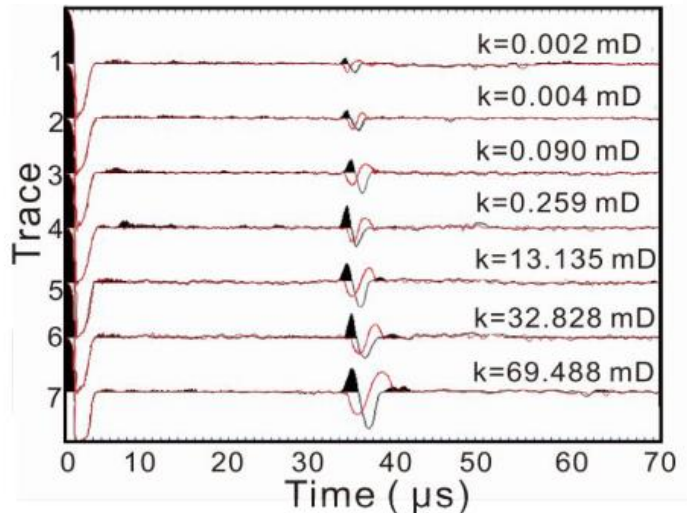
Signals at 10 kHz; P1 = black, P2 = red



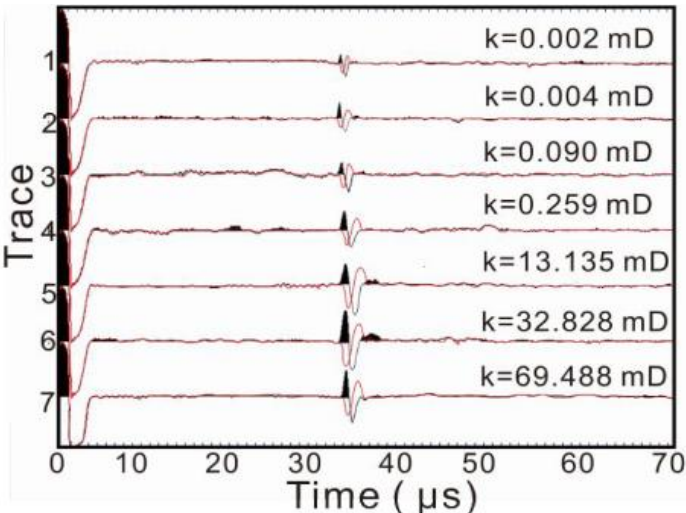
Signals at 500 kHz; P1 = black, P2 = red



Signals at 10 kHz; V1 = black, V2 = red



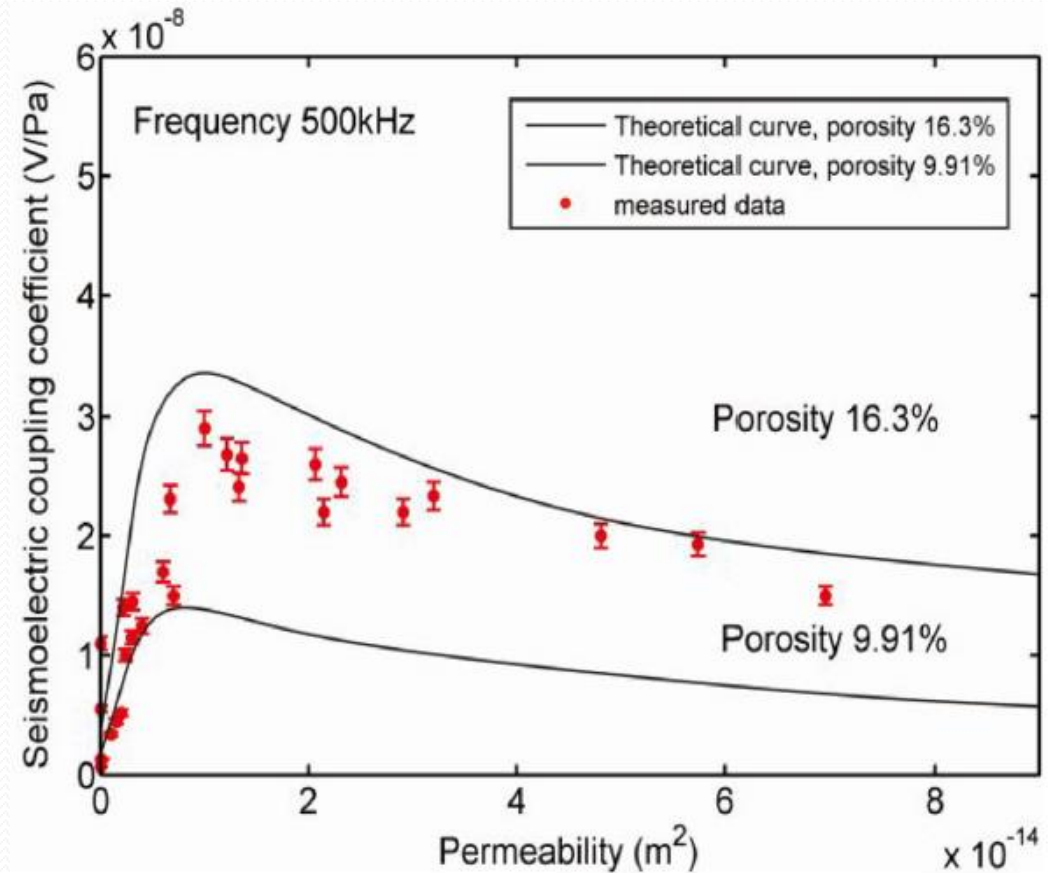
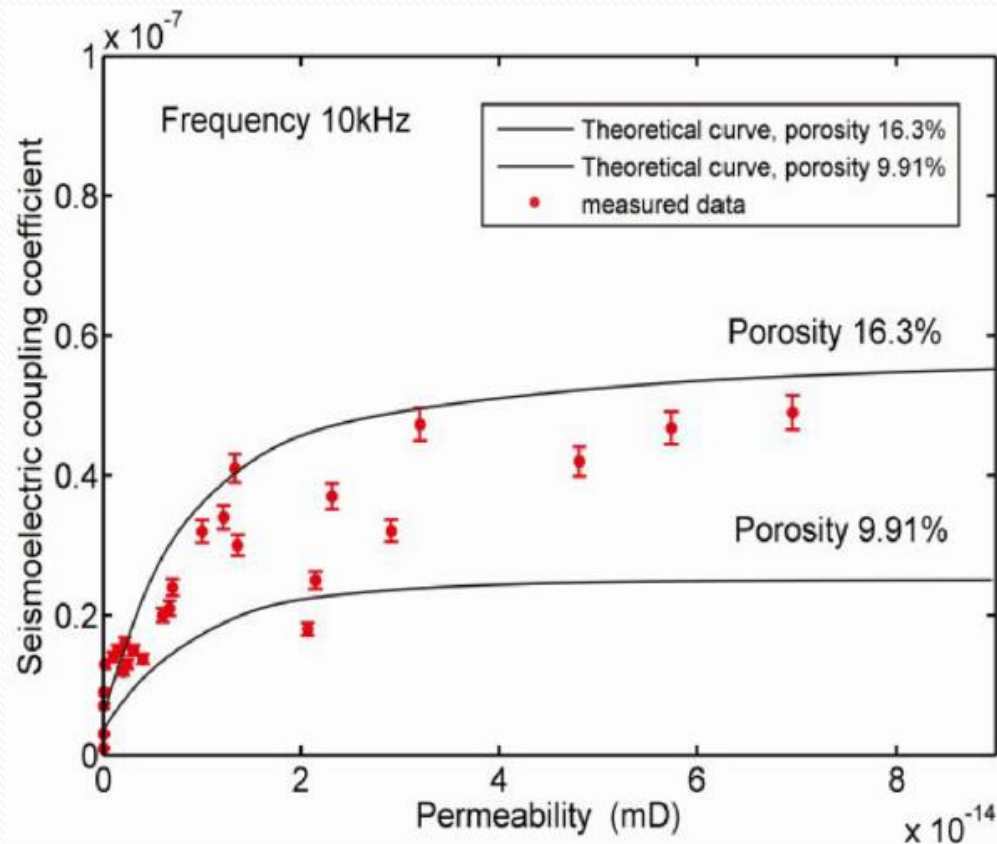
Signals at 500 kHz; V1 = black, V2 = red



The pressure and potential signals recorded at the proximal and distal transducers for frequencies of 10 kHz and 500 kHz

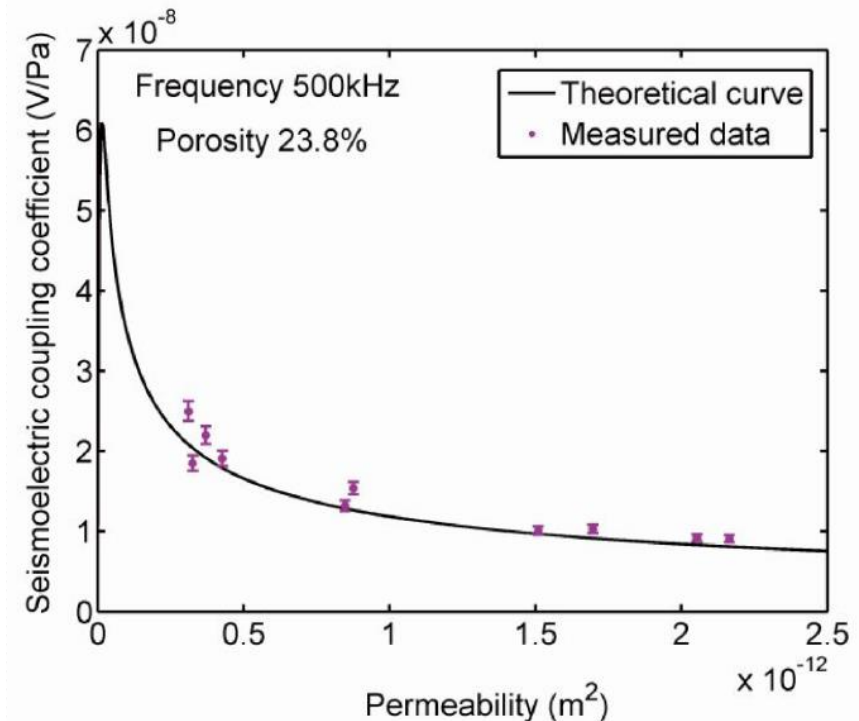
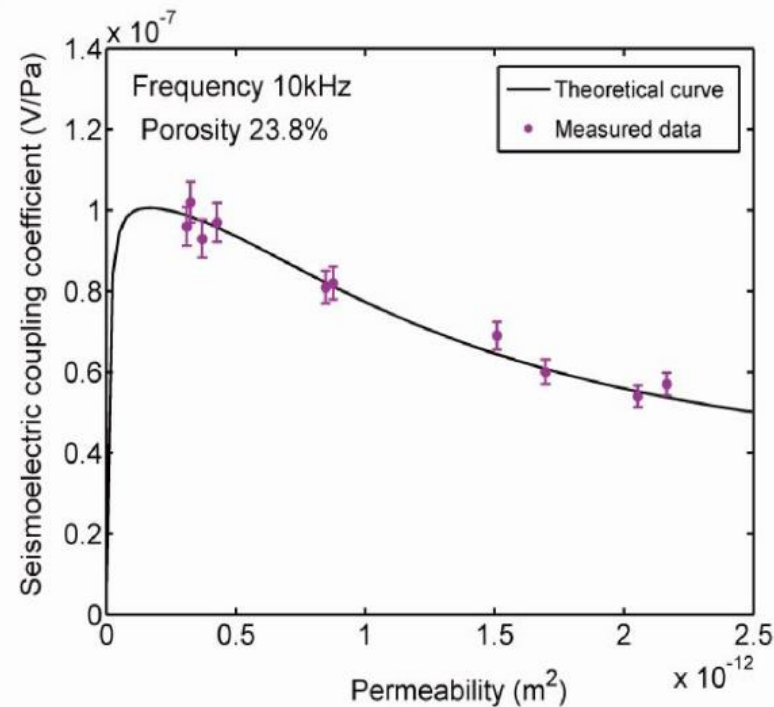
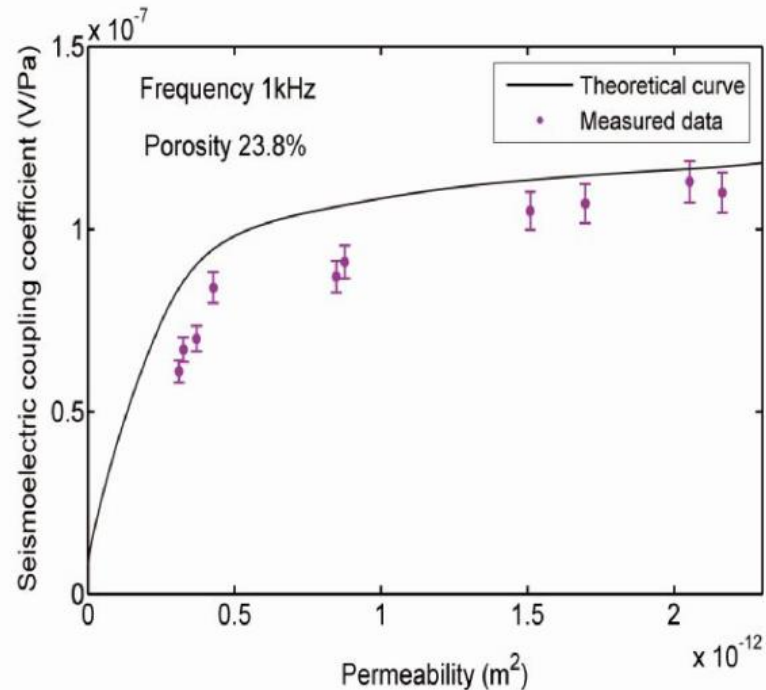
Experimental Results on Natural Rocks with Variable Porosity

Seismoelectric coupling coefficients follow the expected relationship with permeability despite their different porosities (between 9.91% and 16.3%) and consequently agree with modelling for frequencies of both 10 kHz and 500 kHz



Experimental Results on Synthetic Rocks with Fixed Porosity

For synthetic rocks, where the porosity can be controlled, the seismoelectric coupling coefficients follow the expected relationship with permeability and consequently agree with modelling for frequencies of both 10 kHz and 500 kHz, and are approximately correct at 1 kHz.



- We have investigated the effects of permeability and porosity on the seismoelectric conversion using both experimental measurements and theoretical analysis.
- We measured the seismoelectric conversion using 28 rock sample samples with porosities in the range 9.91% - 16.3% and four artificial sandstones with constant porosity equal to 23.8%.
- We have also developed and implemented the capillary bundle model to calculate the seismoelectric coupling coefficient as a function of porosity, permeability and frequency theoretically.
- Experimental and theoretical analyses show that both porosity and permeability affect seismoelectric conversion and present a quantitative dependence between permeability and the seismoelectric coupling.

- Both experimental and theoretical analyses of seismoelectric coupling indicate that seismoelectric conversion is stronger for high porosity rocks across a wide frequency range.
- But the effects of permeability on seismoelectric coupling are complex and can be divided into two permeability regions where $4.05 \times 10^{-15} \text{ m}^2$ (4.05 mD) is the permeability demarcation point:
 - below this permeability value (unconventional reservoirs), the seismoelectric coupling enhances with the increase of permeability; and
 - over this value (conventional reservoirs), the seismoelectric coupling increases first and then decreases with the increase of permeability.

- Dependency of the seismoelectric coupling on permeability is different for different frequencies.
 - At low frequencies (1 kHz) both the natural and artificial samples show that seismoelectric conversion is enhanced by increases in permeability, with the greatest sensitivity in the lower frequency range.
 - At higher frequencies (10–500 kHz), there is a great increase in seismoelectric conversion with increasing permeability, but the seismoelectric conversion reaches a peak and then declines rapidly, especially at the higher frequencies.
- The quantitative relationship between permeability and the seismoelectric coupling is dependent on the frequency and permeability range, based on this quantitative relationship, the permeability can be inferred by the seismoelectric conversion.

Summary

...Putting it all together.

- ❖ Combinations of experimental approaches ...
- ❖ Combination of experiment and modelling ...
- ❖ Combination of frequencies ...
- ❖ Combinations of different types of sample ...

... all allow more in-depth analysis of electro-kinetic and seismo-electric phenomena

- Glover, P.W.J., 2015. Geophysical Properties of the Near Surface Earth: Electrical Properties. Treatise on Geophysics: Second Edition. pp. 89-137.
- Glover, P.W.J., 2018. Modelling pH-Dependent and Microstructure-Dependent Streaming Potential Coefficient and Zeta Potential of Porous Sandstones, *Transport in Porous Media*, vol. 124, no. 1, pp. 31-56.
- Glover, P.W.J. and Déry, N., 2010. Streaming potential coupling coefficient of quartz glass bead packs: Dependence on grain diameter, pore size, and pore throat radius. *Geophysics*, 75(6), pp. F225-F241.
- Glover, P.W.J. and Jackson, M.D., 2010. Borehole electrokinetics. *Leading Edge (Tulsa, OK)*, 29(6), pp. 724-728.
- Glover, P.W.J. and Walker, E., 2009. Grain-size to effective pore-size transformation derived from electrokinetic theory. *Geophysics*, 74(1), pp. E17-E29.
- Glover, P.W.J., Walker, E., Jackson, M.D., 2012a. Streaming-potential coefficient of reservoir rock: a theoretical model. *Geophysics* **77**(2), D17–D43. <https://doi.org/10.1190/GEO2011-0364.1>
- Glover, P.W.J., Ruel, J., Tardif, E. and Walker, E., 2012b. Frequency-dependent streaming potential of porous media - Part 1: Experimental approaches and apparatus design. *International Journal of Geophysics*, 2012.
- Glover, P.W.J., Walker, E., Ruel, J. and Tardif, E., 2012c. Frequency-dependent streaming potential of porous media - Part 2: Experimental measurement of unconsolidated materials. *International Journal of Geophysics*, 2012.
- Peng, R., Di, B., Glover, P.W.J., Wei, J., Lorinczi, P., Ding, P., Liu, Z. (2019 -in press 1), The effect of rock permeability and porosity on seismo-electric conversion: Experiment and analytical modelling, *Geophys J. Int.*
- Peng, R., Di, B., Glover, P.W.J., Wei, J., Lorinczi, P., Ding, P., Liu, Z. (2019 -in press 2), Seismo-electric conversion in shale: Experiment and numerical modelling, *J. Geophys. Res.*
- Peng R., Di, B., Wei, J., Glover, P.W.J., Lorinczi, P., Ding, P., Liu, Z., 2018a, The seismoelectric coupling in shale, 80th EAGE Conference and Exhibition 2018 Proceedings, EAGE, 11 Jun .
- Peng R., Glover, P.W.J., Di, B., Wei, J., Lorinczi, P., Ding, P., Liu, Z., 2018b, The effect of rock permeability and porosity on seismoelectric conversion, 80th EAGE Conference and Exhibition 2018 Proceedings. EAGE. 11 Jun 2018 Publisher URL DOI
- Packard, R. G., 1953. Streaming potentials across glass capillaries for sinusoidal pressure. *The Journal of Chemical Physics*, 21(2), pp. 303–307, 1953.
- Pride, S., 1994. Governing equations for the coupled electromagnetics and acoustics of porous media, *Phys. Rev. B*, 50(21), 15678-15696.
- Revil, A. and Glover, P., 1997. Theory of ionic-surface electrical conduction in porous media. *Physical Review B - Condensed Matter and Materials Physics*, 55(3), pp. 1757-1773.
- Revil, A. and Glover, P.W.J., 1998. Nature of surface electrical conductivity in natural sands, sandstones, and clays. *Geophysical Research Letters*, 25(5), pp. 691-694.
- Revil, A., Pezard, P.A. and Glover, P.W.J., 1999. Streaming potential in porous media 1. Theory of the zeta potential. *Journal of Geophysical Research: Solid Earth*, 104(B9), pp. 20021-20031.
- Tardif, E., Glover, P.W.J. and Ruel, J., 2011. Frequency-dependent streaming potential of Ottawa sand. *Journal of Geophysical Research: Solid Earth*, 116(4).
- Walker, E. and Glover, P.W.J., 2010. Characteristic pore size, permeability and the electrokinetic coupling coefficient transition frequency in porous media. *Geophysics*, 75(6), E235–E246.
- Walker, E. and Glover, P.W.J., 2018. Measurements of the relationship between microstructure, pH, and the streaming and zeta potentials of sandstones. *Transport in Porous Media*, 121(1), pp. 183-206.
- Walker, E., Glover, P.W.J. and Ruel, J., 2014. A transient method for measuring the DC streaming potential coefficient of porous and fractured rocks. *Journal of Geophysical Research: Solid Earth*, 119(2), pp. 957-970.

Leeds
University
Petro
physics

